Analysis of chaining structures in colloidal suspensions subjected to an electric field

G. Bossis,[1] C. Métayer,[1] and A. Zubarev[2]
[1]*Laboratoire de Physique de la Matière Condensée, Université de Nice, Parc Valrose, 06108 Nice Cedex 2, France*
[2]*Department of Applied Mathematics, Ural State University, pr. Lenina, Yekaterinburg, 620083, Russia*
(Received 12 December 2006; revised manuscript received 26 April 2007; published 3 October 2007)

Structures formed by a colloidal suspension of silica particles in 4-methyl cyclohexanol have been analyzed in the presence of an electric field. The formation of chains of particles was detected using an elliptical mirror to collect scattered light and a nearly matched refractive index between particles and solvent. A numerical method has been developed to obtain the size distribution of chains and their kinetics of formation from the record of a two-dimensional map of scattered light. We have compared the experimental size distribution to the prediction of a statistical theory based on a minimization of the free energy of a gas of chains. This theory quite well reproduced the experimental results for small chains but overestimates the tail of the distribution at high field. A saturation of the average size of chains versus the electric field was observed experimentally instead of a continuous growth as would be expected from aggregation under dipolar forces. A kinetic model, taking into account both capture and escape rates of a particle at the extremity of a chain, was shown to reproduce well the experimental growth of the average size of chains with time.

DOI: 10.1103/PhysRevE.76.041401 PACS number(s): 82.70.Dd, 47.57.eb, 42.25.Fx

I. INTRODUCTION

The theory of the liquid state has progressed a lot, thanks to the concept of local structure, which characterized the organization of molecules around a reference one. The pair distribution function $g(r)$ is the basic tool which serves to describe this local structure. When the molecules interact through an isotropic potential (like the Lennard-Jones one), we only have to consider the probability to find another particle at a distance r from the reference one. The problem becomes more difficult in the presence of an anisotropic potential like the dipolar one. The pair distribution function $g(r,\theta)$ is now anisotropic, and many theories have been derived in order to predict this function from knowledge of the energy of the interaction between two spherical dipolar particles [1,2]. The comparison with experiments is not simple since dipolar molecules are not spherical—they have at least two atoms—and taking into account this anisotropy would still complicate the theory a lot. The simplest realization of a dipolar fluid made of spherical entities is actually a suspension of spherical colloidal particles carrying a permanent dipolelike ferrofluid or also colloidal particles polarized by an electric or a magnetic field. In this paper we are dealing with the second kind of suspensions, also known as electrorheological fluids when the change of structure under the applied field is large enough to strongly increase the viscosity of the suspension. Actually our main interest is not the change of viscosity or a test of theories about dense dipolar liquid, but an analysis of the change of structure at low volume fractions in the presence of an external field. At low volume fraction and in the presence of strong dipolar interactions, the pair distribution function is no longer an adequate tool to describe the structure of the suspension. The situation is closer to the one described by aggregation theories where we consider the formation of small clusters which can grow due to the attractive dipolar interactions or be destroyed due to Brownian motion [3]. In this case the structure of the suspension is better characterized by a size distribution of chains containing n particles: $g_n(E)$ for a given applied field E. Our aim in this work was to determine experimentally this size distribution and to compare it with the predictions of statistical theories. Previous theories concerning the equilibrium state of aggregation in the presence of dipolar forces [4–7] differ in the way they calculate the free energy of a gas of chains and also in the consideration of interactions between chains of particles. In this paper we shall present a derivation of the equilibrium size distribution where we discard interactions between the chains of spheres. As we shall see in Sec. IV B, this approximation is justified for the low volume fractions we are going to consider experimentally. Concerning the kinetics of chain formation most approaches are based on irreversible aggregation with the use of the standard Smoluchowski equation [8] and cluster-cluster aggregation model [8–10] predicting a power law for the growth of average size versus time. Other models [11] consider each particle as a sink surrounded by a homogeneous cloud of particles which diffuse towards the sink according to Fick's equation; this kind of model can only predict the evolution in time of the concentration of isolated particles, but not the size distribution. We propose in Sec. II B a model based on the reversible Smoluchowski's equation which can predict the kinetics of growth towards an equilibrium state corresponding to the minimization of the free energy of the system. Comparisons with experiments are very scarce because of the difficulty to obtain experimentally the size distribution of particles. Most papers deal with the observation of chains by optical microscopy of micron-sized spheres with the field parallel to the glass plates. These particles are only slightly Brownian, and the regime studied is the one of irreversible aggregation [12]. Furthermore, the chains of particles settle quite quickly and associated microflow or density gradients can disturb the aggregation process. From light scattering it is possible to get information on the aggregation process of smaller particles which do not sediment, but it is indirect information, often difficult to interpret in terms of the size of aggregates. A first possibility is to relate turbidity measurements to the average

 ©2007 The American Physical Society

length of aggregates [13], but it supposes that all the aggregates have the same length. Instead of the transmitted light we can record the scattered light in order to have more complete information on the structure. Such an approach on a system of quasimatched silica spheres has already been used to study the kinetics of the coarsening of dipolar chains [14]. In this paper we focus on the early stage of chain formation, where transverse coarsening can be neglected, and also on the relation between chain formation and the interparticle potential. As was demonstrated for magnetic particles, light scattering under the action of an external field can be used to measure the repulsive force between colloidal particles [15]. In a preceding paper [16] we presented a device able to collect scattered rays in a half space and an example of what could be deduced about chain formation in an electric field from the record of the scattered light. In this paper we propose a theory aiming to predict the size distribution of chains and their kinetic of formation and we compare these predictions with experimental data. Section II is devoted to the theory of chain formation under the action of an external field dealing with both the prediction of the equilibrium size distribution and kinetics of growth. In Sec. III we briefly describe the experiment and explain the analysis of the scattered pattern through an inverse method [17], giving the size distribution of chains and the distance between particles inside the chains. Last, in Sec. IV we present experimental results obtained from this inverse analysis and compare them to the predictions of the models presented in Sec. II for both the equilibrium structure and its dynamic of growth. We conclude with a brief discussion about possible developments of this work to characterize interparticle forces in the presence of an applied external field.

II. CHAIN FORMATION IN THE PRESENCE OF DIPOLAR COLLOIDS

In this theoretical section we shall present a general view of chain formation through dipolar interactions. The first part, devoted to the equilibrium size distribution of chains, is also relevant to the case of particles having a permanent dipole like, for instance, in ferrofluid. The second part concerns the kinetics of chain formation when the field is turned on and is more specific to the response time of electrorheological or magnetorheological fluids.

A. Equilibrium size distribution

First of all, we suppose that each particle has acquired the same electrical dipole moment; that is to say, it is not modified by the local field of other dipoles. This means, in particular, that we ignore any interactions between the chains. Second, we suppose that each particle only interacts with its nearest neighbors in the chain.

We call g_n^0 the equilibrium number of n-particle chains per unit volume of the suspension, and our purpose is to determine this function for every integer n.

To this end we write the free energy per unit volume of the system as follows:

$$F = kT\sum_{n=1}^{\infty} g_n^0\left(\ln\frac{g_n^0\mathbf{v}}{e} - \ln z_n\right), \quad e = 2.72\ldots\ . \tag{1}$$

Here $\mathbf{v}$ is the volume of a particle and z_n is the configuration integral of n particles belonging to a given chain. The first term in the brackets on the right-hand side of Eq. (1) corresponds to the entropy of an ideal gas of chains due to their translational motion. The second term is the internal free energy of the n-particle chain which contains both entropy and energy of the chain contrarily to the previous models [16].

The equilibrium distribution function g_n^0 should provide a minimum of the free energy F under the condition of conservation of the total number of particles per unit volume:

$$\sum_{n=1}^{\infty} n g_n^0 = \frac{\varphi}{\mathbf{v}}. \tag{2}$$

Here φ is the total volume fraction of the particles in the suspension and $\varphi/\mathbf{v}$ the number of particles per unit volume.

Minimizing Eq. (1) under the condition (2), we get

$$g_n^0 = \frac{1}{\mathbf{v}} z_n \Lambda_a^n, \tag{3}$$

where Λ_a is an unknown Lagrange multiplier. In order to determine this multiplier one needs to substitute Eq. (3) into the balance equation (2). Before we have to calculate the chain configuration integral z_n of a chain of n particles.

In order to determine z_n we consider the total configuration integral Z_n of n particles in any position:

$$Z_n = \frac{1}{\mathbf{v}^n}\int \exp\left(-\frac{1}{2}\sum_{i\neq j} u(\mathbf{r}_{ij})\right) d\mathbf{r}_2 d\mathbf{r}_3 \cdots d\mathbf{r}_n, \quad \mathbf{r}_{ij} = \mathbf{r}_i - \mathbf{r}_j. \tag{4}$$

Here $\mathbf{r}_i$ is the radius vector of the ith particle and $u(\mathbf{r}_{ij})$ is the dimensionless potential of the interaction between the ith and jth particles.

The integral (4) includes all mutual positions of the n particles, and not only configurations corresponding to a linear chain. By using the well-known virial expansion method, we can write Z_n in the form of a combination of integrals of the Mayer function $f(r) = -1 + e^{-u(r)/kT}$:

$$\frac{1}{\mathbf{v}}\int d\mathbf{r}, \tag{5}$$

$$\frac{1}{\mathbf{v}^2}\int f(\mathbf{r})d\mathbf{r}, \quad \frac{1}{\mathbf{v}^3}\int f(\mathbf{r}_{12})f(\mathbf{r}_{23})d\mathbf{r}_{12}d\mathbf{r}_{23},$$

$$\frac{1}{\mathbf{v}^4}\int f(\mathbf{r}_{12})f(\mathbf{r}_{23})f(\mathbf{r}_{34})d\mathbf{r}_{12}d\mathbf{r}_{23}d\mathbf{r}_{34}, \ldots .$$

The first integral in (5) corresponds to an ideal gas of noninteracting particles. Since the Mayer function tends to zero rapidly when the distance r between two interacting particles increases and, therefore, correlations between these particles decreases, the second integral in Eq. (5) corre-

sponds to clusters of two particles. The integrand in the third term in (5) significantly differs from zero when the correlations between the first and second, second and third particles are not weak. Thus this integral corresponds to clusters of three particles. The same considerations show that the fourth term of (5) corresponds to a chain of four particles, etc. Note that in (5), only terms containing multiplications of nearest particles are included. We do not consider terms like $f_{12}f_{13}f_{23}$, $f_{12}f_{13}f_{23}f_{14}$, etc., since only linear clusters are considered here; whereas terms like $f_{12}f_{13}f_{23}$ correspond to closed rings, terms like $f_{12}f_{13}f_{23}f_{14}$ describe bulk or branched structures.

The situation where all n particles belong to the same chain corresponds to the integral

$$\frac{1}{\mathbf{v}^{n-1}}\int f(\mathbf{r}_{12})f(\mathbf{r}_{23})\cdots f(\mathbf{r}_{n-1,n})d\mathbf{r}_{12}d\mathbf{r}_{23}\cdots d\mathbf{r}_{n-1,n}, \quad (6)$$

and only this integral will contribute to z_n in Eq. (1) since the other ones correspond to configurations where the n particles are not inside the same chain.

The integration in (6) is the product of $n-1$ similar integrals, but we must also take into account that if we consider a particle i and integrate on the position of particle $i+1$, the integration should only take place on an half upper space since the half lower space is occupied by particle $i-1$. Therefore, the configuration integral of the n-particle chain has the following form:

$$z_n = \left(\frac{1}{2\mathbf{v}}\int f(\mathbf{r})d\mathbf{r}\right)^{n-1}, \quad (7)$$

where the integration should be carried out over all space. It should be noted that this form of the configuration integral z_n is a direct consequence of the "nearest-neighbor" approximation and thus, it is not surprising that the configuration integral is given by a power of the second virial coefficient of the interacting particles in the chain.

Combining Eqs. (7) and (3), we come to the following expression for the equilibrium distribution function:

$$g_n^0 = \frac{1}{\mathbf{v}}X^n \exp(-w),$$

$$w = \ln\left(\frac{1}{2\mathbf{v}}\int f(\mathbf{r})d\mathbf{r}\right), \quad X = \Lambda \exp(w). \quad (8)$$

Substituting expression (8) into the conservation equation (2) gives an equation for X:

$$\frac{X}{(1-X)^2} = \varphi \exp(w)$$

or

$$X = \frac{1+2y-\sqrt{1+4y}}{2y},$$

where

$$y = \varphi \exp(w). \quad (9)$$

Equations (8) and (9) give the final result for the equilibrium distribution functions g_n^0 of a gas of chains in the "nearest-neighbor" approximation.

The equilibrium mean number of particles in the chain is

$$\langle n\rangle^0 = \frac{\varphi}{\mathbf{v}\sum_{n=1}^{\infty} g_n^0},$$

and using expression (8) we get

$$\langle n\rangle^0 = \varphi \exp(w)\frac{(1-X)}{X}. \quad (10)$$

In order to calculate w in Eq. (8) we need to know the Mayer function and therefore the interaction potential between two particles.

We consider monodisperse spherical particles carrying a dipolar moment m and suspended in a fluid of dielectric permittivity ε_f. The particles are supposed to be surrounded by thin double electrical layers, which screen the attractive van der Waals interaction between the particles.

The dipolar interaction energy, normalized by kT is,

$$u_{dd}(r,\theta) = \frac{\lambda}{2r^3}(1-3\cos^2\theta),$$

where

$$\lambda = \frac{2\mathrm{m}^2}{4\pi\varepsilon_0\varepsilon_f \mathrm{d}^3\mathrm{kT}}. \quad (11)$$

Here θ is the angle between the field $\boldsymbol{E}$ and radius vector $\boldsymbol{r}$; $d=2a$ is the diameter of the particles, and r is the distance between the centers of the two particles normalized by d. This definition of λ corresponds to dipoles aligned with the field and is appropriated to study dipolar aggregation.

For the dimensionless potential of electrostatic interaction between two spherical particles, surrounded by thin double electrical layers, we took [18]

$$u_c(r) = -\frac{Q^2}{8\pi\varepsilon_0\varepsilon_1 a^3 kT}\frac{1}{\kappa^2}\ln\{1-\exp[-\kappa 2a(r-1)]\}. \quad (12)$$

Here Q is the charge of the particle surface (the charge of the motionless part of the double layer) and $1/\kappa$ is the Debye-Huckel thickness of the ionic double layer.

The total dimensionless potential of interaction between these particles is

$$u(r,\theta) = u_{dd}(r,\theta) + u_c(r). \quad (13)$$

Using Eq. (13) one can calculate numerically the coupling parameter w [Eq. (8)] and therefore the equilibrium size distribution g_n^0.

B. Kinetics of the chain formation

Let us turn now to the study of time evolution of an ensemble of chains. We consider an initially homogeneous sus-

pension and the field is switched on at $t=0$. As we shall see later, in the condition of our experiments, the concentration of the chains and their hydrodynamic mobility are significantly less than those for the single particles and so we have considered only the "chain-particle" aggregation, neglecting the "chain-chain" aggregation as well as any interactions between the chains.

First, we will obtain an equation for the flux of single particles arriving on a chain—i.e., the number of single particles "adsorbed" by a chain per unit of time—using the classical approach described by Fuchs [19]. Then we will express the growth of a chain expressed as a balance between this adsorption and the escape flux due to Brownian motion.

1. Flux of dipolar particles towards a sink

We consider a chain consisting of n particles surrounded by free particles and suppose that the free particles only join the chain at its extremity. Let c_∞ be the concentration of the free particles at infinite distance from the chain and $c(\boldsymbol{r})$ the local concentration of these particles at the point $\boldsymbol{r}$. Since the attraction between a chain and free particles, in this approximation, is the same as the attraction between two single particles, we consider the kinetics of formation of a doublet. One of the particles of the doublet will be considered as free and the other as fixed in the space. The fixed particle in our approximation corresponds to the particle at the extremity of a chain.

The diffusion equation of free particles in the presence of the dimensionless attractive energy $u(\mathbf{r})$ is

$$\frac{\partial c}{\partial t} = \nabla[D(\mathbf{r})\nabla c] + \nabla[D(r)c\nabla u(\mathbf{r})]. \tag{14}$$

Here $D(r)=D_0\psi(r)$, where D_0 is the usual coefficient of diffusion of an isolated particle and $\psi(r)$ takes into account the hydrodynamic interaction between two particles; in the first order versus the separation, we have $\psi=1-3d/4r$ [20]. The boundary conditions of Eq. (14) are

$$c \to c_\infty, \quad r \to \infty,$$

$$c \to 0, \quad r \to d. \tag{15}$$

Equation (14) does not have any analytical solution; in order to get such solutions, two kinds of approximations are done [11]. First, as the time needed to establish a stationary concentration profile around the sink is short in comparison to the time needed to change c_∞, we can write Eq. (14) in the quasistationary approximation

$$\nabla[D(\mathbf{r})\nabla c] + \nabla[D(r)c\nabla u(\mathbf{r})] = 0. \tag{16}$$

Second, we average the attractive part of the noncentral dipole-dipole potential over the angles

$$\bar{u}_{dd} = -\frac{\lambda}{2x^3}\frac{\int_{S_{\text{attr}}}(3\cos^2\theta - 1)d(\cos\theta)}{\int_{-1}^{1} d(\cos\theta)}. \tag{17}$$

Here $x=r/d$ and S_{attr} is the surface of the unit sphere corresponding to an attractive energy ($|\cos\theta| > 1/\sqrt{3}$); note that the same expression applies for a sink which is a single particle and for a chain since the two particles at the extremities have the same S_{attr} than a single one. Finally we get

$$\bar{u}_{dd}(r) = -\frac{\lambda d^3}{3\sqrt{3}r^3}. \tag{18}$$

Now instead of Eq. (16) we have

$$\nabla[D(r)\nabla c] + \nabla[D(r)c\nabla\bar{u}(r)] = 0, \quad \bar{u} = \bar{u}_{dd} + u_c. \tag{19}$$

In a spherical coordinate system with the origin at the center of the fixed particle, this equation has the following form:

$$\frac{\partial}{\partial r}\left[D_0\psi(r)r^2\left(\frac{\partial c}{\partial r} + \frac{\partial}{\partial r}\bar{u}(r)\right)\right] = 0. \tag{20}$$

Equation (20) directly leads to the following expression for the flux J of the free particles toward the attractive sink [21]:

$$J = Ac_\infty,$$

$$A = \frac{4\pi D_0 d}{W}, \quad W = \int_1^\infty \frac{\exp[\bar{u}(x)/kT]}{\psi(x)x^2}dx. \tag{21}$$

2. Time evolution of an ensemble of chains

Now we have all the ingredients to calculate the time evolution of the system of chains. Let g_n be the number of n-particle chains in a unit volume of the system. By definition, $g_1=c_\infty$. Our aim now is to derive and solve the kinetic equations for g_n. We will take into account that the following two processes take place simultaneously during the chain formation. The first one is the adsorption of free particles at the extremity of the chains, which has been considered in the previous part, and the second process is the desorption of particles at extremity due to Brownian motion. As the energy of interaction of the particles at the ends of the chain is smaller than the energy of "internal" particles—approximately by a factor of 2—it seems reasonable to consider only the "evaporation" of the particles located at the extremity of the chain and to neglect other kinds of rupture. Since the "adsorption" of a free particle by the n-particle chain transforms the chain into an $(n+1)$-particle chain and the "evaporation" of the terminal particle transforms an n-particle chain into an $(n-1)$-particle chain, we come to the following kinetic equation:

$$\frac{\partial g_n}{\partial t} = -Ag_1(g_n - g_{n-1}) + B(g_{n+1} - g_n), \quad n > 1. \quad (22)$$

Here A is the adsorption coefficient given by Eq. (21) and B the escape coefficient which will be determined below. This kind of equation was already used in another context for living polymers, but with an important difference related to the fact that living polymers can break anywhere along the chain [22].

The equation for g_1 has the following form:

$$\frac{\partial g_1}{\partial t} = -2Ag_1^2 - Ag_1\sum_{n=2} g_n + B\left(2g_2 + \sum_{n=3} g_n\right). \quad (23)$$

In Eq. (23) we take into account, first, that when two single particles gather to form a doublet, their relative hydrodynamics mobility is twice the relative mobility between an individual particle and a motionless chain and second that, when a doublet disappears, two new free particles appear.

One can show that the system of equations (22) and (23) automatically satisfies the following balance condition:

$$\sum_{n=1} ng_n = C, \quad (24)$$

where C should be equal to the total concentration $\varphi/\mathbf{v}$ of particles in the suspension.

Now we have to determine the escape coefficient B. For this purpose, let us determine the stationary solution g_n^0 of the system of equations (22) and (23), which corresponds to the equilibrium state of the system. One can easily verify that the following distribution function satisfies Eqs. (22) and (23) when the left-hand term is zero:

$$g_n^0 = \frac{B}{A}Y^n, \quad (25)$$

where Y is an undetermined parameter. On the other hand, the approach, based on minimization of the free energy of the system, leads to Eq. (8) for the equilibrium distribution function. Obviously, both ways, the kinetics and thermodynamics ones, must give the same result for the equilibrium distribution function.

Equating the results (8) and (25), we get

$$Y = X, \quad B = A\exp(w). \quad (26)$$

In order to handle the sums appearing in Eq. (23) we introduce a new variable $N=\Sigma_{n=1}g_n$, which is the total number of chains (including the monomers) in the suspension. The total number of chains will decrease only if isolated particles adsorb on any other chain, and it will increase if any chain, except of course isolated particles, desorbs one particle. Rewriting Eqs. (22) and (23) with this new variable gives the following set of equations:

$$\frac{\partial N}{\partial t} = -Ag_1N + B(N - g_1),$$

$$\frac{\partial g_1}{\partial t} = -Ag_1^2 - Ag_1N + B(g_2 + N - g_1),$$

$$\frac{\partial g_2}{\partial t} = -Ag_1(g_2 - g_1) + B(g_3 - g_2),$$

$$\frac{\partial g_3}{\partial t} = -Ag_1(g_3 - g_2) + B(g_4 - g_3), \quad (27)$$

with initial conditions at $t=0$: $g_1=N=\frac{\varphi}{\mathbf{v}}$, $g_2=g_3=\cdots=0$.

The average number of particles per chain will be

$$\langle n\rangle(t) = \frac{\varphi}{\mathbf{v}N(t)}. \quad (28)$$

The system of equations (27) can be solved numerically. The main problem is that it contains an infinite number of equations. In order to break this infinite chain of equations, one can take into account that if the number n is significantly larger than the equilibrium number $\langle n\rangle^0$ of particles in the chains, the corresponding chain concentration g_n must be very small. Thus one can choose a certain maximal number n_{max} ($n_{max} > \langle n\rangle^0$) of particles in the chains and put $g_n=0$ for $n > n_{max}$. The value of n_{max} is determined by the desirable accuracy and the computation time. We have used $n_{max}=10$.

Before applying this model, we have to see how the size distribution of chains can be obtained from the light scattering experiment. This experiment was already described in a preceding paper [16], so here we shall focus more on the analysis of the data and on the procedure used to obtain the size distribution of chains and the interparticle distance between particles.

III. CHAIN STRUCTURE FROM INVERSE ANALYSIS OF THE STRUCTURE FACTOR

Light scattering is currently used to obtain information either on the size and shape of particles or on spatial organization of particles inside colloidal suspensions. For instance, the determination of size distribution of colloidal particles is realized on commercial instruments by recording the light scattered in different directions on several photodiodes (about 70) disposed both at low and large scattering angles. The intensity of the light scattered at different angles is then used as input of a least-squares method based on a theoretical scattered intensity expressed as a function of the weights of the size distribution. Different numerical schemes allow us to determine the size distribution, but the refractive indices of the particles and of the suspending liquid need to be rather close in order to avoid multiple scattering.

In our case we have used monodisperse silica particles with a diameter of 400 nm dispersed in 4-methylcyclohexanol. A silane coating molecule, the trimethoxysilyl-propylmethacrylate, was used to ensure a good stability of the dispersion. The refractive index of the particles is close to the one of the suspending fluid ($n_f = 1.457$, $n_p = 1.44$) so that the simple Rayleigh-Gans-Debye (RGD) theory can be applied without too much error. For the case of a chain of N particles we have compared the intensity calculated using the many-particle Mie scattering calculation [23] to the usual approximation given by

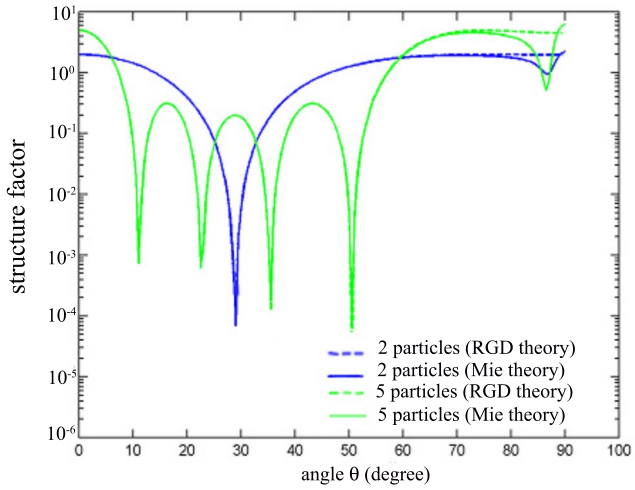

FIG. 1. (Color online) Comparison between Rayleigh-Gans-Debye and multiple Mie scattering for a five-sphere chain (gray) and a two-sphere chain (black).

$$I_n(\mathbf{q}) = F(\mathbf{q})S_n(\mathbf{q}) = F(\mathbf{q})\left(n + \sum_{i=1}^{n}\sum_{j=1,j\neq i}^{n} e^{i\mathbf{q}\cdot r_{i,j}}\right), \quad (29)$$

where $F(\mathbf{q})=\frac{3}{u^3}(\sin u - u\cos u)$ with $u=\mathbf{q}\cdot a$ ($\mathbf{q}$ is the modulus of the scattering wave vector defined by the difference of incident and scattered wave vectors, $\mathbf{q}=\mathbf{k}_i-\mathbf{k}_d$, $k=2\pi n_f/\Lambda$, with $\Lambda=632.8$ nm and a the radius of the particles). We can see in Fig. 1 that the only visible difference is at large angles and still the difference remains low. So in the following we shall only use the RGD model to describe the scattered pattern.

We shall also neglect multiple scattering between chains, an approximation justified by the small refractive index contrast and the quite low volume fraction used. In this approximation the total intensity scattered by chains of different lengths will be just the sum of intensities scattered by each chain:

$$I^{\text{th}}(\mathbf{q}) = \sum_n a_n F(\mathbf{q})S_n(\mathbf{q}), \quad (30)$$

where a_n is the number of chains containing n particles in the scattering volume. The experimental structure factor is quite easy to obtain experimentally since in the absence of field the scattered intensity is proportional to the form factor and can be used to normalize the scattered intensity in the presence of field, so that the total structure factor is

$$S(\mathbf{q},E) = \sum_n a_n S_n(\mathbf{q}) = \frac{I(\mathbf{q},E)}{I(\mathbf{q},0)}. \quad (31)$$

This procedure of normalization is valid since the low volume fraction in our experiment allows us to neglect the structure factor at zero field. It avoids difficult corrections such as those related to the dependence of the scattering volume as a function of angle, reflected rays at interfaces, or defects and impurities of the optical glasses. The experimental apparatus consists of an ellipsoidal mirror, with the cell

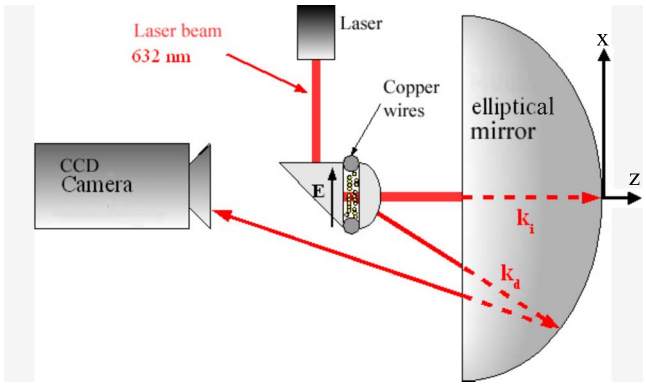

FIG. 2. (Color online) Experimental setup: the chains are aligned on the x axis. Note that the dimension of the cell is only one centimetre compared to a radius of ellipsoidal mirror of 30 cm.

placed at the first focus of the mirror and the objective of a video camera placed at the second focus (Fig. 2). This ellipsoidal mirror and the presence of a hemispherical lens (BK7 glass with refractive index $n_g=1.515$) as a constitutive part of the cell to avoid refraction at the glass air interface allow us to collect all angles scattered in a cone of a half angle of 70°5. The experimental information consists of a set of points related to the intensity collected on each pixel of the video camera. We wish to determine the ensemble of coefficients a_n representing the size distribution of chains. Calling P the number of pixels, we have to minimize the quantity

$$\chi^2 = \sum_{i=1}^{P} [\mathbf{S}^{\text{expt}}(\mathbf{q}_i) - \mathbf{S}^{\text{th}}(\mathbf{q}_i)]^2. \quad (32)$$

The theoretical structure factor of a chain of n particles contains at least one parameter which is the average distance between two neighbor particles inside a chain. For a rigid chain of n particles regularly spaced of a distance d along the x axis with $\mathbf{k}_i$ along the z axis and $\mathbf{k}_d$ defined by the polar and azimuthal angles θ, ϕ, we have

$$S_n^{\text{th}}(\theta,\varphi) = n + 2\sum_{j=1}^{n-1} j\cos[kd(n-j)\sin(\theta)\cos(\varphi)]. \quad (33)$$

A picture of the structure factor of a rigid chain of ten particles is shown in Fig. 3(a). The vertical central line would extend to infinity for a set of perfectly aligned scatters. The width of this line is inversely proportional to the length of the chain. The two arcs on the side are first-order interferences between the particles spaced by a distance d. The angle $\theta_{\max}$ between the center of the figure ($\theta=0$) and the center of one arc in the perpendicular direction gives the average distance between particles through the Bragg relation: $\sin\theta_{\max}=\Lambda/(\langle d\rangle n_g)$. Note that n_g is the refractive index of the hemispherical lens and not of the fluid; it comes from the use of Snell's law at the fluid-glass interface. With our wavelength $\Lambda=632.8$ nm and the maximum observable value of $\theta=70°5$, we are limited to distances larger than

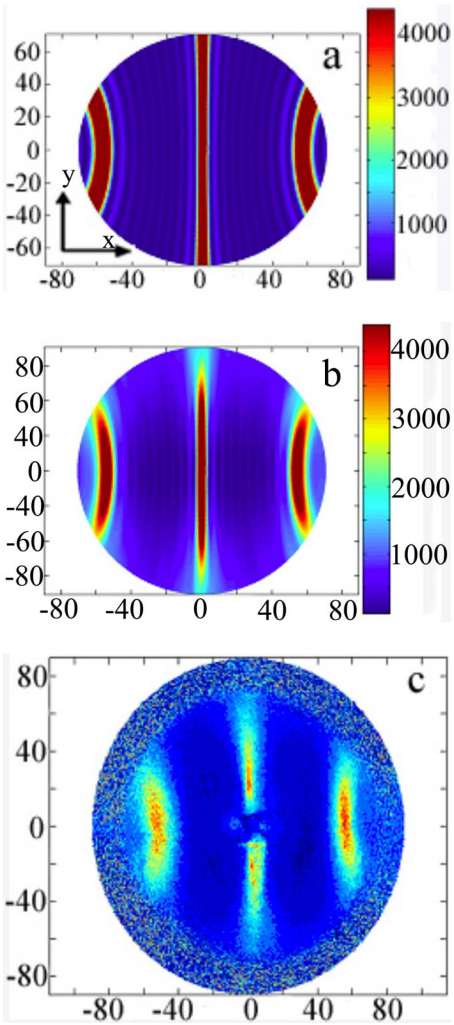

FIG. 3. (Color online) (a) Structure factor of chains whose particle's positions are aligned on a straight line with constant separation (chains of ten particles). (b) Structure factor of chains whose particle's positions are simulated through Monte Carlo method (chains of ten particles, $\lambda=5$) (reproduced from Ref. [16]). (c) Experimental structure factor: volume fraction $\varphi=3\%$ and field $E=2.5$ kV/cm. The angles on the horizontal and vertical axes correspond to the ones defining the angular positions of the projection of $\mathbf{k}_d$, respectively, on the field axis and perpendicular to it.

440 nm and that is more than the diameter of the particles (400 nm). Actually by using the aisle of the Bragg peak it is possible to access distances until 420 nm; for lower distances, we have used neutron scattering.

In practice, these chains are not rigid and the position of each particle fluctuates inside the chains. It is quite important to take into account these fluctuations if we want to have a good determination of the size distribution of chains. For instance, we can see, by comparing Figs. 3(a) and 3(b), that the structure factor of a rigid chain [Fig. 3(a)] is quite different from the one of a Brownian one [Fig. 3(b)]. For the Brownian case, the positions of the particles were derived from a Monte Carlo simulation with hard spheres plus a dipolar interaction characterized by an already high value of the coupling parameter ($\lambda=5$). Despite this quite high value the residual motion of the particles has a noticeable effect on the structure factor and the result is more similar to the experimental one [Fig. 3(c)] than to the case of a rigid chain. It is then necessary to introduce some parameters describing the random motion of particles inside the chain. The structure factor S_n of a cluster of n particles reads

$$\langle S_n(\theta,\varphi)\rangle = n + 2\frac{\int \sum_{i=1}^{n}\sum_{j=i+1}^{n} \cos(\mathbf{q}\cdot\mathbf{r}_{ij})P(\mathbf{r}_{ij})\prod d\mathbf{r}_{ij}}{\int P(\mathbf{r}_{ij})\prod d\mathbf{r}_{ij}}, \tag{34}$$

where $P(\mathbf{r}_{ij})$ is the Boltzmann probability to find a distance $\mathbf{r}_{ij}$ between the pair i,j. For a chainlike cluster we can decompose the separation vector between two particles i and j inside the chains as $\mathbf{r}_{ij}=(j-i)\langle d\rangle+\mathbf{r}^{\mathrm{per}}+\mathbf{r}^{\mathrm{par}}$, where $\mathbf{r}^{\mathrm{per}}$ and $\mathbf{r}^{\mathrm{par}}$ are the random shifts from the equilibrium position, respectively, perpendicular and parallel to the axis of the chain and $\langle d\rangle$ the average distance between two neighbor particles in the direction of the field. We suppose that these random displacements can be represented by a Gaussian probability of standard deviation, respectively, σ^{per} and σ^{par}. This is a reasonable approximation since the equilibrium position is close to the minimum of potential energy and the expansion of the Boltzmann factor around this minimum would give a quadratic term for the dependence on position. The structure factor of a chain of n particles is given by an integral over the positions of each pair of particles [specified by $(j-i)\langle d\rangle$, r^{par}, r^{per}, γ] multiplied by the two Gaussian functions $P_{\parallel}$ and $P_{\perp}$. The angle $\gamma=\gamma_i-\gamma_j$ is the difference of cylindrical angle in the plane perpendicular to the chain axis and has a constant probability. Neglecting the correlations of position in the plane perpendicular to the axis of the chain, Eq. (34) can be transformed into

$$\langle S_n(\theta,\varphi)\rangle = n + 2\sum_{j=1}^{n-1} j\frac{\int_{-\infty}^{+\infty}\int_{-\infty}^{+\infty}\int_{0}^{\pi}\cos[((n-j)\mathbf{q}\cdot\langle\mathbf{d}\rangle+\mathbf{q}\cdot\mathbf{r}^{\mathrm{per}}+\mathbf{q}\cdot\mathbf{r}^{\mathrm{par}})]P_{\perp}(r^{\mathrm{per}})P_{\parallel}(r^{\mathrm{par}})r^{\mathrm{per}}dr^{\mathrm{per}}dr^{\mathrm{par}}d\gamma}{\pi\int_{-\infty}^{+\infty}\int_{-\infty}^{+\infty}P_{\perp}(r^{\mathrm{per}})P_{\parallel}(r^{\mathrm{par}})r^{\mathrm{per}}dr^{\mathrm{per}}dr^{\mathrm{par}}}. \tag{35}$$

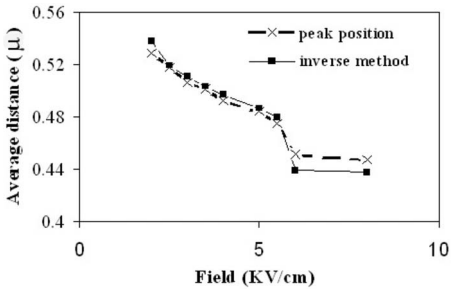

FIG. 4. Average distance $\langle d\rangle$ between particles vs applied electrical field for the suspension with the particle volume concentration $\varphi=0.1$. Line with crosses presents calculations from Bragg formula $\langle d\rangle=\Lambda/(n_g \sin\theta_{\max})$; the line with squares presents results obtained from Eq. (35) and the minimization procedure, described in the Appendix.

The three quantities $\langle d\rangle$, σ^{per}, and σ^{par} were considered as parameters related to the form factor of the chain and their influence on the scattering image is quite different from the effect of the size distribution coefficients. It is then possible to decouple the minimization of the set of parameters a_n from the three form factors. The derivation of the coefficients a_n and of the three parameters $\langle d\rangle$, σ^{per}, and σ^{par} is described in the Appendix. Basically we first minimize χ^2 relatively to a_n, keeping constants the values of $\langle d\rangle$, σ^{per}, and σ^{par}. Then we keep constant the values of a_n that we have found and minimize the three parameters. This procedure is iterated until we get converging values.

IV. EXPERIMENTAL RESULTS AND COMPARISON WITH THEORY

In the first part we are going to deduce the parameters of the interparticle potential from the measurement of the distance between particles in a chain; then, in the second section we shall use this interaction potential to calculate the size distribution and compare it to the one deduced from light scattering. In the same way, we will, in the third part, compare the theory with experiment for the kinetics of chain formation.

A. Interparticle distance

The average interparticle distance $\langle d\rangle$ versus the applied electric field can be either obtained directly from the angular position $\theta_{\max}$ of the maximum intensity on the ring [cf. Fig. 3(c)] using $\sin\theta_{\max}=\Lambda/n_g\langle d\rangle$ or from the whole calculation where it is taken as a free parameter together with σ^{per} and σ^{par} as described in Sec. III. The comparison between the two determinations is shown in Fig. 4 for the highest volume fraction ($\varphi=10\%$). First, we can see that the two determinations are very close, except at the highest fields where the direct method gives a higher distance. Actually for the highest fields the peak position is just on the rim of the image and its precise position is difficult to guess without using the fitting procedure. The second observation is that we have a sudden drop of interparticle distance between $E=5$ and 6 kV/cm. We are now going to try to model this behavior. We can calculate the average distance between nearest neighbors in the approximation of pairwise interactions. The mean distance along the chain axis between the centers of two particles is given by a Boltzmann average

$$\langle d\rangle = \frac{\int r\cos\theta \exp[-u(r,\theta)]r^2 dr d\cos\theta}{\int \exp[-u(r)]r^2 dr d\cos\theta}. \tag{36}$$

Both integrals as well as their ratio in Eq. (36) diverge since the Boltzmann exponent $\exp[-u(\mathbf{r})]$, where $u(r)$ is the energy normalized by kT, tends to unity when the distance r between the particles increases. Actually, if two neighbor particles far from the reference one do not interact with it, it should not be included in the integral. If the potential hole defined by $u(r,\theta)$ is deep enough, it is possible to approximate it by a fourth-order expansion around its minimum value; therefore, the potential energy is well approximated around its minimum and its divergence when the distance increases prevents the particle from escaping from the well. This approximation is acceptable if $\lambda \gg 1$ which is not verified in our case, since for the lowest field $E=1.5$ kV/cm we have $\lambda \sim 2$. A more natural way to calculate this average distance is to remain in the reciprocal space, since we record the angular dependence of the scattered light, and to look for the distance giving a maximum in scattered intensity:

$$S(\theta) = 1 + 2\frac{\int_a^R \cos[kr\sin(\theta)]\exp - u(r)dr}{\int_a^R \exp - u(r)dr}. \tag{37}$$

Here $k=2\pi n_g/\Lambda$. In Eq. (37) we use for the upper limit R of integration a value satisfying $kR\sin(\theta)=p2\pi$ with p an integer and θ the scattering angle. This choice avoids short period oscillations of $S(\theta)$ due to long-range correlations. In that way, the result converges quickly when increasing the value of p. We then detect the maximum $\theta_{\max}$ of $S(\theta)$, and the average distance is therefore $\langle d\rangle=\Lambda/(n_g \sin\theta_{\max})$. Another way would be to use the Mayer function $\exp[-u(r)]-1$ instead of the Boltzmannn function. The result is almost identical except at the lowest values of λ where it overpredicts by a few percent. The results shown in Fig. 5 were based on the use of Eq. (37). For the choice of the potential energy $u(r)$, we took Eq. (13) representing a short-range Debye-Huckel repulsion and a long-range attractive dipolar energy. This latter was deduced from measurements of the dielectric constant of the suspension. At a frequency of 10 kHz we obtained $\lambda=0.98E^2$ with E in kV/cm. The repulsive part still depends on two parameters: the Debye-Huckel screening length $1/\kappa$ and the charge of the particles, $Q=Zq_e$, q_e being the charge of the electron. In practice, it was not possible to determine these two parameters from our limited range of separation distances; for instance, we see in Fig. 5 that $Z=10\,500$ and $\kappa=1.13\times10^8$ fits as well as $Z=2500$ and $\kappa=0.8\times10^8$. Using the O'Brien-White [24] numerical

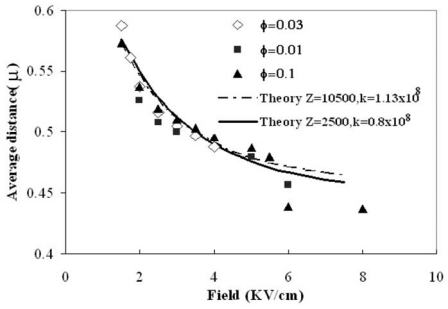

FIG. 5. Average distance $\langle d \rangle$ between particles vs applied electric field. Comparison between experiment (■, $\varphi=0.01$; ◇, $\varphi=0.03$; ▲, $\varphi=0.1$) and theory using a Debye-Huckel potential [Eq. (12)] with $Z=2500$, $\kappa=0.8\times10^8$ (solid line) and $Z=10500$, $\kappa=1.13\times10^8$ (dash-dotted line).

procedure we can relate the charge to the zeta potential. For instance, for the first set we obtain $\zeta \approx 10$ mV and still less for the second one. We have tried to measure the value of the zeta potential with a zetasizer (Malvern) equipped with U cell but the uncertainty in this nonaqueous solvent was too high to help us choose a better set of parameters. In any event, thereafter we just need a good representation of the potential and we shall see that both sets of parameters predict the same values for the size distribution of chains or for the time evolution of the structure. It is also worth noting that the sudden drop of distance cannot be explained in terms of the usual Debye-Huckel and dipolar interactions as can be seen in Fig. 5. On the other hand, we have verified that, for a gap of about 0.07 diameter where the change of slope begins, the order of magnitude of the van der-Waals attractive force remains completely negligible in comparison to the repulsive one. It is known that the dipolar approximation strongly underestimates the attractive force and a multipolar expansion could be used for a better prediction if the polarizability were only characterized by the bulk permittivity of the particles. Unfortunately, in our system the frequency dependence of the dielectric constant shows that the polarizability is dominated by ionic motion and we are not aware of any model able to predict the attractive force between two double layers polarized by a strong external field.

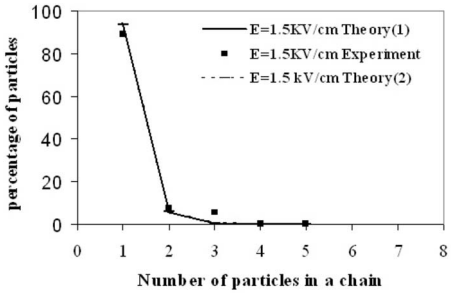

FIG. 6. Percentage of particles belonging to a chain of size n for $E=1.5$ kV/cm and a volume fraction $\varphi=0.03$. Solid squares are for experiment. The solid line labeled "Theory(1)" is the theoretical prediction [Eq. (37)] with the set of parameters $Z=2500$ and $\kappa=0.8\times10^8$ for $u(r)$. The dashed line, labeled "Theory(2)," is obtained with the other set of parameters $Z=10\,500$ and $\kappa=1.13\times10^8$.

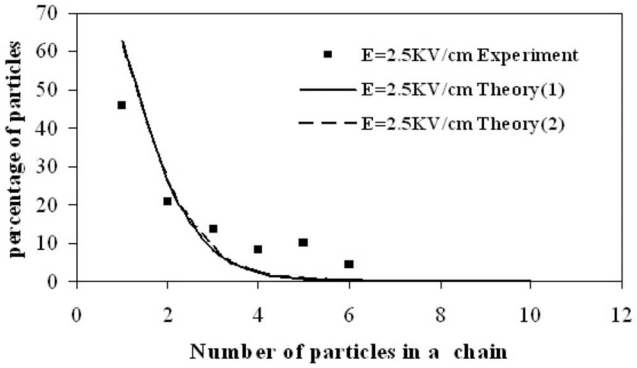

FIG. 7. Percentage of particles belonging to a chain of size n, $E=2.5$ kV/cm; same legend as in Fig. 6.

B. Size distribution of chains

Knowing the energy of interaction between two particles which is given by Eqs. (11)–(13) with $Z=2500$, $\kappa=0.8\times10^8$, and $\lambda=0.98E^2$ (E in kV/cm), we are now able to predict the average size distribution of chains from Eqs. (8) and (9). Furthermore, it is worth stressing that any choice of parameters (Z,κ) able to fit the change of distance between particles (Fig. 5) will predict the same size distribution; it is shown in Figs. 6–8 where the two theoretical curves referring, respectively, to set (1) $Z=2500$, $\kappa=0.8\times10^8$ and (2) $Z=10\,500$, $\kappa=1.13\times10^8$ are almost undistinguishable. The experimental size distribution is obtained as explained in the Appendix. In Figs. 6–8 we present the comparison between experiment and theory for three values of the field: $E=1.5$, 2.5, and 3.5 kV/cm and a volume fraction $\varphi=0.03$. We have plotted the percentage of particles belonging to a chain of size n ($n=1$ corresponds to isolated particles). We see that about 90% of the particles are still isolated at $E=1.5$ kV/cm, and it falls to about 50% at $E=2.5$ kV/cm. For these two fields the agreement between the theory and the experiment is quite fair, especially if we recall that there is no free parameter in the model. On the contrary, for the field $E=3.5$ kV/cm, there is a quite important disagreement for isolated particles that experimentally remain at 40% whereas

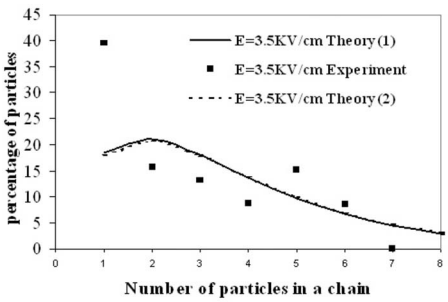

FIG. 8. Percentage of particles belonging to a chain of size n, $E=3.5$ kV/cm; same legend as in Fig. 6.

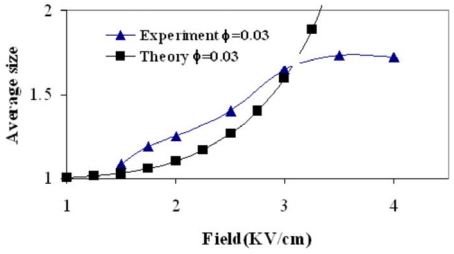

FIG. 9. (Color online) Average size of the chains versus electric field for a volume fraction $\varphi=0.03$ (▲, experiment; ■, theory).

the theory predicts that only 15% of particles should remain isolated. Also the model predicts the existence of a tail in the distribution that corresponds to the existence of long chains of particles. The fact that we do not observe this tail experimentally is not due to a limitation of the inverse analysis of light scattering: using a Monte Carlo simulation of chain formation to calculate the scattering image, we are well able to recover by inverse analysis the tail of the size distribution. Furthermore, when we plot the average size of clusters versus the electric field in Fig. 9, we see that the behavior of the experimental and theoretical curves are quite different: experimentally the average size reaches a plateau $\langle n\rangle=1.6$ for fields larger than 3.5 kV/cm, whereas the model predicts an average size that steadily grows with the electric field. We also find this leveling of the average size with the electric field for the two other volume fractions ($\varphi=0.01$ and $\varphi=0.1$) that we have studied. The reason for this behavior is not clear; it could be related to the motion of ions around the particles caused by the applied electric field, which could induce a local convection able to break the longer chains. Another cause of the difference between our theory based on isolated chains and the experiments at $E=3.5$ kV/cm could come from the coarsening of the structure with the agglomeration of side chains in a body-cubic-tetragonal (bct) structure which, for example, is described in [14]. As the scattered light gives information in the reciprocal space, the thickening of structures perpendicularly to the electric field will give rise to a peak in the direction of the electric field. In our sample we actually begin to see a small peak in this direction at an angle of 43° for a field of 3.5 kV/cm (cf. Fig. 10). This beginning of coarsening could explain partly the disagreement between experiment and theory that we observe for this field in Fig. 8.

Another interesting piece of information is related to the dynamics of chain formation. The dynamics of chain formation is recorded with a standard charge-coupled device (CCD) camera at the rate of 25 images per second; in this case, the information contained in each image is more noisy than the ones used for the equilibrium situation where the light intensity was averaged over a few seconds. Nevertheless, we have verified that the size distribution and the average size obtained at equilibrium within 1/25 s were about the same as the one obtained by averaging the intensity of each pixel during several seconds. The evolution with time of the average size of chains is given by Eq. (28) with $N(t)$ obtained from the numerical solution of Eq. (27). In Fig. 11 we compare this theoretical prediction to the experimental

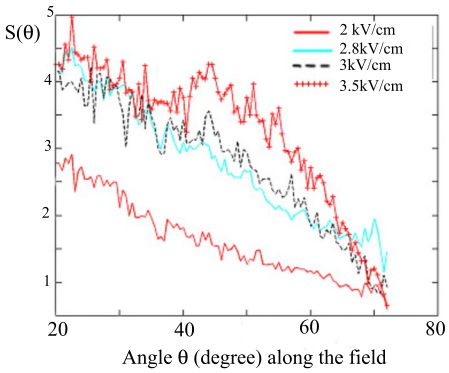

FIG. 10. (Color online) Structure factor along the direction of the field (x axis of Figs. 2 and 3) for different field values, from bottom to top: 2 KV/cm; 2.8 KV/cm; 3 KV/cm; 3.5 KV/cm.

one for a volume fraction $\varphi=0.03$ and a field $E=3$ kV/cm. The agreement is very good, and this is proof that the dynamics of growth of chains of Brownian particles in the presence of dipolar interactions is well captured by our model. The importance of Brownian motion in slowing down the kinetics of growth is well demonstrated by comparing with a former theory of irreversible aggregation of particles under an electric field [8]. In this other model, at each step of aggregation all the chains have the same size and the time needed to double their size is the one needed for two equal chains to move on the average distance separating them in the field direction. The force between two chains is calculated from the sum of dipolar interactions between all the particles belonging to these chains. The resulting kinetics for the average size is [8]

$$\langle n(t)\rangle = \sqrt{\frac{3\phi}{C}t+1},$$

with

$$C = 2\pi\frac{\eta a^3}{kT\lambda}. \tag{38}$$

In Eq. (38), η is the viscosity of the suspending fluid and λ the coupling parameter [cf. Eq. (11)]. Both the rate of aggre-

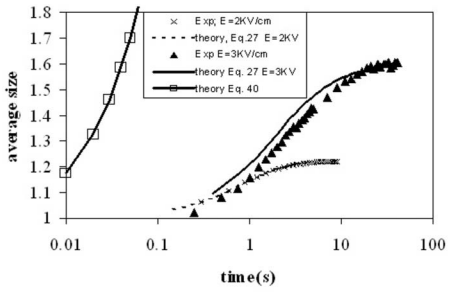

FIG. 11. Average size of chains versus time after turning on the field at a frequency $f=10$ kHz for $E=3$ kV/cm, ▲, and for $E=2$ kV/cm, ×; solid and dotted lines represent the theory [cf. Eq. (28)], respectively, for $E=3$ kV/cm and $E=2$ kV/cm. Open squares with solid line represent the prediction of Eq. (38) without Brownian motion.

gation and the shape of the curves predicted by Eq. (38) are very different from the experimental one as can be seen in Fig. 11; it demonstrates that even with a dipolar force dominating the Brownian one ($\lambda=9$ for $E=3$ kV/cm) the influence of Brownian forces remains dominant in the kinetics of chain's formation. The ability of our model to reproduce the kinetics of growth is also confirmed at a lower field: $E=2$ kV/cm. Nevertheless, we must mention that the value of the escape rate B was adjusted to predict the experimental equilibrium value at large time instead of using Eq. (27) since it is only at 3 kV/cm that the theory predicts the right equilibrium value (cf. Fig. 9).

V. CONCLUSION

The aim of this paper was twofold. First, we wanted to show that, from an analysis of scattered light, it was possible to get a size distribution of elongated objects, and second, we wanted to establish a model capable of describing the first step of chain formation in a colloidal dispersion submitted to an electric field. The first task was facilitated by the uniform orientation of the chains that are aligned along the field, but it would not have been possible without the use of the elliptical mirror which allows us to gather information in a wide solid angle. An improvement of this system is under study to adapt it on a rheometer. Note that it could be used to obtain the size distribution of rodlike particles if they were first oriented by the application of an electric (or a magnetic) field. Of course, the entire numerical treatment of the scattered image can apply to neutron scattering, giving access to smaller sizes of particles. Concerning the interactions between spherical particles, the measurement of the distance between two neighbor particles allows us to get direct information on the interaction energy in the presence of a high field. This information is crucial, for instance, in explaining the mechanisms leading to the giant electrorheological effect with nanoparticles [25]. Our analysis of the kinetics of chain formation captures well the experimental result because both adsorption and desorption at the extremity of the chain determine the kinetics of growth as long as the average size of the chain is not too large (typically $n<100$ or $\boldsymbol{\lambda}<20$). For larger $\boldsymbol{\lambda}$ the number of equations becomes too important and furthermore we expect a lateral growth of the chains which could not be accounted for by this model.

ACKNOWLEDGMENT

One of us (A.Z.) is grateful to the Russian Fund of Fundamental Investigations for financial support of this work.

APPENDIX: MINIMIZATION OF χ^2 [EQ. (32)]

We have to solve the two sets of equations

$$\frac{\partial \chi^2}{\partial a_n}=0, \tag{A1}$$

$$\frac{\partial \chi^2}{\partial p_i}=0, \tag{A2}$$

where $i=1,3$.

The first one is a minimization relative to the weights of the size distribution and the second one are the three parameters ($\langle d\rangle$, σ^{per}, σ^{par}) appearing in Eq. (35).

Each set of equations is solved in the same way, using the method that we are going to describe for the parameters of the size distribution, a_n.

We define the vector $\mathbf{a}=(a_1,a_2,\ldots,a_n)$, and we are looking for a vector $\delta\mathbf{a}$ such as the new vector, $\mathbf{a}'=\mathbf{a}+\delta\mathbf{a}$ cancels all the partial derivative of χ^2.

Using a second-order Taylor expansion we have

$$\chi^2(\mathbf{a}')=\chi^2(\mathbf{a})+\sum_{n=1}^{N}\frac{\partial\chi^2(\mathbf{a})}{\partial a_n}\delta a_n+\frac{1}{2}\sum_{n,l=1}^{N}\frac{\partial^2\chi^2(\mathbf{a})}{\partial a_n\,\partial a_l}\delta a_n\delta a_l+\cdots, \tag{A3}$$

with N the maximum size that we consider. If we note

$$[\mathbf{A}]_{nl}=\sum_{n,l=1}^{N}\frac{\partial^2\chi^2(\mathbf{a})}{\partial a_n\,\partial a_l}$$

and

$$[\mathbf{b}]_n=-\frac{\partial\chi^2(\mathbf{a})}{\partial a_n},$$

Eq. (A3) reads

$$\frac{\partial\chi^2}{\partial a_n}(\mathbf{a}')=\mathbf{A}\cdot\delta\mathbf{a}-\mathbf{b}.$$

Since the ensemble of partial derivative of χ^2 must be equal to zero, we get

$$\mathbf{a}'=\mathbf{a}+\mathbf{A}^{-1}\cdot\mathbf{b},$$

where the elements of $\mathbf{A}$ and $\mathbf{b}$ only depend on the values of the derivative of χ^2 for the old values $\mathbf{a}$. In order to calculate these partial derivative, the simplest method is to start from a first order Taylor expansion of S^{th},

$$S^{\mathrm{th}}(q,\mathbf{a}')\approx S^{\mathrm{th}}(q,\mathbf{a})+\sum_{\mathrm{n}=1}^{\mathrm{N}}\frac{\partial S^{\mathrm{th}}(q,\mathbf{a})}{\partial a_n}\delta a_n$$

$$\equiv S^{\mathrm{th}}(q,\mathbf{a})+\sum_{n=1}^{\mathrm{N}}X_n(q,\mathbf{a})\,\delta a_n,$$

and to consider that $S^{\mathrm{expt}}(q)-S^{\mathrm{th}}(a_{\mathrm{old}},q)$ is a constant. The change $\Delta\mathbf{a}$ that must be added to the old value $\mathbf{a}$ is then obtained, solving

$$\alpha\,\Delta\mathbf{a}=\beta, \tag{A4}$$

with $\alpha_{\mathrm{nl}}=\Sigma_{i=1}^{p}X_n(q_i;\mathbf{a})X_l(q_i;\mathbf{a})$ and $\beta_n=\Sigma_{i=1}^{p}[S^{\mathrm{expt}}(q_i)-S^{\mathrm{th}}(q_i,\mathbf{a})]X_n(q_i,\mathbf{a})$.

This method converges quickly towards the solution only if the initial solution is close to the final one. We have then used the method of Marquardt [26] which takes advantage both of this method and also of the gradient method which quickly converges. The only modification compared to Eq. (A4) is to replace $\boldsymbol{\alpha}$ by $\boldsymbol{\alpha}'$:

$$\boldsymbol{\alpha}' \equiv \boldsymbol{\alpha}_{ij}(1+\zeta) \quad \text{for } i=j \quad \text{and} \quad \alpha_{ij} \text{ for } i \neq j.$$

The parameter ζ must be large when we are far from the minimum and small when we are close. We have chosen to divide ζ by 10 each time the value of χ^2 is decreasing and to multiply it by 10 in the opposite case [27].

This method needs knowledge of some initial values for the separation distance, $\langle d \rangle$ and the coefficients a_n defining the size distribution. We used for the initial value of $\langle d \rangle$ the one deduced from the Bragg relation applied to the apparent angular position $\langle d \rangle = \Lambda / (n_g \sin \theta_{\max})$. The initial values of a_n are obtained from the solution of the linear problem [28,29]. Actually the use of this nonlinear method is not obligatory since, once the value of $\langle d \rangle$ is fixed, the problem becomes linear. Nevertheless, in practice, it is easier to introduce the "non-negativity constraint" on the parameters a_n with this method by taking equal to zero the negative values obtained from the solution of the linear problem. In the case of a large distribution of size of chains, the number of the different classes of size defining the a_n can be quite large and the existence of statistical uncertainty (or systematic error) can easily lead to an almost singular system. It leads to large oscillations of the values of a_n that are clearly unphysical. To overcome this problem we generally apply the minimization not to χ^2 but to $\chi^2 + \lambda_i N_c$, where N_c is related to the amplitude of the oscillations of the a_n, $N_c = \sum_{n=1}^{N-1} (a_{n+1} - a_n)^2$, and λ_i is a Lagrange multiplier. This procedure allows us to choose from all the solutions of the problem the one whose coefficients vary smoothly: in practice, there is a large range of values for λ_i giving a good value of the minimization but for low values of λ_i the parameters a_n show strong oscillations whereas, on the contrary, for high values of λ_i, the distribution is flat. The optimal value of λ_i is obtained by the method of inflection point [30]. In our case the large number of measured angles (120 000) and the strong anisotropy of the scattering figure also helps to stabilize the solution and using only the minimization of χ^2 gives results similar to the one obtained with the minimization of $\chi^2 + \lambda_i N_c$.

Finally we have to impose that the parameters have a positive value and that $\langle d \rangle > 2a$. Each time a parameter is negative, its value is divided by 10; in the same way, if $\langle d \rangle < 2a$, the value of $\langle d \rangle - 2a$ is divided by 10. On the other hand, a robust method like the Gauss-Jordan method needs to be used for the solution of the problem.

[1] J. J. Weis and D. Levesque, Phys. Rev. E **48**, 3728 (1993).
[2] J. J. Weis and D. Levesque, Phys. Rev. Lett. **71**, 2729 (1993).
[3] M. J. Stevens and G. S. Grest, Phys. Rev. E **51**, 5962 (1995).
[4] A. O. Cebers, Magn. Gidrodin. **2**, 36 (1974).
[5] L. Y. Iskakova and A. Y. Zubarev, Phys. Rev. E **66**, 041405 (2002).
[6] J. C. Teixeira, M. A. Osipov, and M. M. Telo da Gama, Phys. Rev. E **57**, 1752 (1998).
[7] P. G. de Gennes and P. A. Pincus, Phys. Kondens. Mater. **11**, 189 (1970).
[8] H. See and M. Doi, J. Phys. Soc. Jpn. **60**, 2778 (1991).
[9] S. Fraden, A. J. Hurd, and R. B. Meyer, Phys. Rev. Lett. **63**, 2373 (1989).
[10] C. Helgesen, A. T. Skjeltorp, P. M. Mors, R. Botet, and R. Jullien, Phys. Rev. Lett. **61**, 1736 (1988).
[11] J. M. Janssen, J. J. M. Baltussen, A. P. Van Gelder, and J. A. A. J. Perenboom, J. Phys. D **23**, 1455 (1990).
[12] J. H. E. Promislow, A. P. Gast, and M. Fermigier, J. Chem. Phys. **102**, 5492 (1995).
[13] S. Cutillas, A. Meunier, E. Lemaire, G. Bossis, and J. Persello, Int. J. Mod. Phys. B **10**, 3093 (1996).
[14] J. E. Martin, J. Odinek, T. C. Halsey, and R. Kamien, Phys. Rev. E **57**, 756 (1998).
[15] F. L. Calderon, T. Stora, O. Mondain Monval, P. Poulin, and J. Bibette, Phys. Rev. Lett. **72**, 2959 (1994).
[16] C. Métayer, V. A. Sterligov, A. Meunier, G. Bossis, and J. Persello, J. Phys.: Condens. Matter **16**, S3975 (2004).
[17] J. S. Pedersen, Adv. Colloid Interface Sci. **70**, 171 (1997).
[18] D. Quemada and C. Berli, Adv. Colloid Interface Sci. **98**, 51 (2002).
[19] N. A. Fuchs, Z. Phys. **89**, 736 (1934).
[20] G. K. Batchelor, J. Fluid Mech. **74**, 1 (1976).
[21] E. J. W. Vervey and J. Th. G. Overbeek, *Theory of Stability of Lyophilic Colloids* (Elsevier, Amsterdam, 1948), p. 166.
[22] M. E. Cates, Macromolecules **20**, 2289 (1987).
[23] D. W. Mackowski and M. L. Mischenko, J. Opt. Soc. Am. A **13**, 2266 (1996).
[24] R. W. O'Brien and L. R. White, J. Chem. Soc., Faraday Trans. 2 **74**, 1607 (1978).
[25] W. Wen, X. Huang, S. Yang, K. Lu, and P. Sheng, Nat. Mater. **2**, 727 (2003).
[26] D. W. Marquardt, J. Soc. Ind. Appl. Math. **11**, 431 (1963).
[27] W. H. Press, B. P. Flannery, S. A. Teukolsky, and W. T. Vetterling, *Numerical Recipes* (Cambridge University Press, Cambridge, England, 1989).
[28] J. Brunner-Popela and O. Glatter, J. Appl. Crystallogr. **30**, 431 (1997).
[29] O. Glatter, J. Appl. Crystallogr. **10**, 415 (1977).
[30] H. Schnableger and O. Glatter, Appl. Opt. **30**, 4889 (1997).